

## ENERGY STORAGE CAPACITY CONFIGURATION OF ELECTRIC VEHICLE CHARGING STATION WITH PV UNDER PEAK SHAVING MODE

Shanshan SHI

State Grid Shanghai Electric Power  
Research Institute – China  
[sss3397@163.com](mailto:sss3397@163.com)

Yang HE

Shanghai University of  
Electric Power – China  
[heyang\\_epiphyllum@163.com](mailto:heyang_epiphyllum@163.com)

Yu ZHANG

State Grid Shanghai Electric Power  
Research Institute – China  
[zhangyu@sh.sgcc.com.cn](mailto:zhangyu@sh.sgcc.com.cn)

Yufei WANG

Shanghai University of  
Electric Power – China  
[energystorage@163.com](mailto:energystorage@163.com)

Hailong BAO

State Grid Shanghai Electric Power  
Research Institute – China  
[baohl@sh.sgcc.com.cn](mailto:baohl@sh.sgcc.com.cn)

Li ZHU

Shanghai University of  
Electric Power – China  
[super\\_jolie@163.com](mailto:super_jolie@163.com)

### ABSTRACT

*To analyse the fast charging load and the intermittent photovoltaic (PV) output power connected to the charging station, we combine the PV output power and electric vehicle (EV) charging power as equivalent load power. The energy storage system (ESS) capacity is configured according to equivalent load for the purpose of peak-shaving. The daily cost of charging station and the root mean square (RMS) of ESS charge-discharge power are taken as objective functions. The ratio of upper and lower limit power of equivalent load to average charging power of EV are taken as decision variables respectively and an ESS capacity configuration model is established. The objective functions are optimized by NSGA-II algorithm with an improved cross distribution index (CDI). The individuals of the first non-dominated layer after the final iteration are selected as optimal solution. According to the distribution of target values, the upper and lower limit powers of grid are determined, and the ESS capacity is calculated. The results show that the minimum cost is needed when ESS capacity is only enough to store intermittent residual PV energy. Meanwhile, the improved CDI based on the logistic function can better realize optimal solution of the algorithm and accelerate convergence speed of the solution in the later stage of evolution.*

### I. INTRODUCTION

The development and popularization of EVs have made the planning of charging infrastructure particularly important [1, 2]. Using PV power to charge EVs directly not only reduces the dependence of EV charging on the grid [3], but also avoids grid voltage fluctuations caused by PV grid-connection. However, the uncertainty of PV output power and charging load leads to instability of grid [4]. In order to take full advantage of solar energy, it is essential to configure appropriate ESS capacity to absorb PV output power, and provide continuous and stable power to the loads [5]. Literature [6] systematically studied the structural design and capacity optimization method of PV-based battery switch station, and provided a theoretical basis for the operation of PV-based battery

switch station. The self-consumption ability of PV under different charging power level is analysed in literature [7], which shows that the self-consumption ability is decreasing with the charging power level increasing and more grid power need to supply EVs. Therefore, it is indispensable to configure ESS in PV charging stations to coordinate energy flow [8]. In literature [9], the battery of EVs is used as an ESS to study the control and charging management strategies of the PV system, which can effectively coordinate the power transmission within the system. As one of the methods to guide the orderly charging of EVs, time-of-use electricity price can be used to realize load optimization [10]. The charging cost of EVs can be reduced through managing the energy of PV and ESS to realize the economic operation of the charging station based on the time-of-use electricity price in [11,12]. In [13], an improved decision-tree-based algorithm is proposed to reduce the peak load in residential distribution networks by coordinating with EVs, PV units and ESS.

By establishing the equivalent model of EV random charging load and PV output power, the ESS can be utilized to exert the peak-shaving effect on the equivalent load owing to the schedulability of the ESS. Considering the daily cost of the charging station as the economic indicator, the RMS of ESS charge-discharge power is used as the load optimization indicator and the rationality of the model can be evaluated. The ESS capacity is calculated according to the decision variables of the first non-dominated layer of the algorithm. In the genetic operation of the algorithm, the logical function is used to change the CDI, and the superiority and rapidity in finding solutions are compared.

### II. THE OPERATION STRATEGY OF CHARGING STATION

#### A. System Structure

The charging station can be divided into following six units: distribution network system, EES, PV system, energy management system (EMS), AC/DC converter and DC/DC converter. Energy flowing and information transferring among the units are shown in Figure 1.

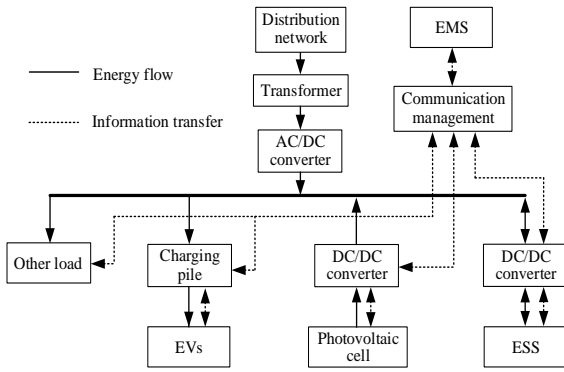


Fig. 1 Structure of PV integrated EV charging station

### B. Charge-discharge Strategy of ESS

In the charging station, PV power as a supplement is directly converted to the grid for EVs charging and reduces the power demand from the grid. So the PV power and the EV charging load can be combined as the equivalent load power, which springs from the grid. As ESS has the function of coordinating energy flowing among energy units, it can be used to adjust the power of the equivalent load, which is shown in Figure 2.

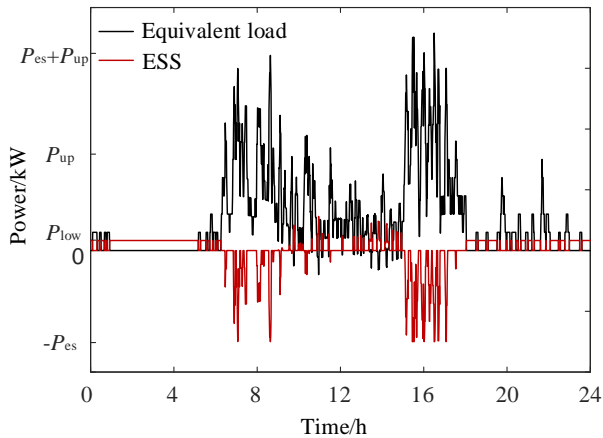


Fig. 2 Power curve of equivalent load and ESS

Set the upper limit power of the equivalent load as  $P_{up}$ , the lower limit power of the equivalent load as  $P_{low}$  and the rated power of ESS as  $P_{es}$ . When the equivalent load power is larger than  $P_{up}$ , ESS shall discharge to satisfy the requirement of excessive load power requirements, and the purpose of load peaking is achieved. If the equivalent load power is larger than  $P_{es} + P_{up}$ , the excessive load will be rejected for charging service, When the equivalent load power is less than  $P_{low}$ , the ESS will be charged to achieve the purpose of valley load filling. Through the charge-discharge strategy of the ESS, the peak-to-valley difference of the equivalent load is reduced and the power supplied by the grid is stabilized between reasonable upper and lower limit.

## III. MULTI-OBJECTIVE ESS CAPACITY CONFIGURATION

### A. Optimal Object

#### (1) The cost of charging station

The cost of the charging station mainly consists of the initial construction cost, operation and maintenance cost, ESS investment cost and electricity purchasing cost, which are calculated as equation (1) to (4):

$$C_1 = (C_{cs} + C_{pv} + C_{pile}) \times \frac{r(1+r)^{m_1}}{(1+r)^{m_1} - 1} \quad (1)$$

$$C_2 = k_{cs}C_{cs} + k_{es}(C_e E + C_p P_b) \quad (2)$$

$$C_3 = \frac{24}{N} \int_0^{24} P_t x_t dt \quad (3)$$

$$C_4 = (C_e E + C_p P_b) \times \frac{r(1+r)^{m_2}}{(1+r)^{m_2} - 1} \quad (4)$$

Where  $C_1$  is the initial construction equivalent annual cost of charging station, which mainly contains transformer purchasing cost  $C_{cs}$ , PV cost  $C_{pv}$  and the charging piles cost  $C_{pile}$ ;  $r$  is the discount rate;  $m_1$  is the service life of the charging station.  $C_2$  is the operation and maintenance cost;  $C_e$  and  $C_p$  are the unit price of energy storage battery and the unit price of power conversion device;  $E$  and  $P_b$  are the energy storage capacity and the maximum discharging power;  $k_{cs}$  and  $k_{es}$  are the annual operation and maintenance coefficient of the transformer and ESS.  $C_3$  is the electricity purchasing cost;  $P_t$  ( $P_t \leq P_{es} + P_{up}$ ) and  $x_t$  are the equivalent load power and electricity purchasing price at time  $t$ .  $C_4$  is the initial investment equivalent annual cost of energy storage battery,  $m_2$  is the service life of ESS. The cost of one day can be calculated as:

$$C = \frac{C_1}{365} + \frac{C_2}{365} + C_3 + \frac{C_4}{365} \quad (5)$$

#### (2) The RMS of the ESS charge-discharge power

The RMS of ESS charge-discharge power reflects the degree of peak shaving. It can be written in equation (6):

$$D = \frac{1}{2 \times \sqrt{1440}} \sum_{t=1}^{1440} \left\{ \left[ P_t - \lambda_1 P_{ave} + |P_t - \lambda_1 P_{ave}| \right]^2 + \left[ \lambda_2 P_{ave} - P_t + |\lambda_2 P_{ave} - P_t| \right]^2 \right\}^{\frac{1}{2}} \quad (6)$$

Where  $P_{ave}$  is the average charging power of EVs;  $\lambda_1$  and  $\lambda_2$  are the ratio of the upper and lower limit power of the equivalent load to average power respectively.

### B. Constraint Condition

#### (1) The charging time of EV

The demand of EV charging power is uncertain. Assume that initial charging time of the  $k$ th EV is  $t_{ik}$  and the

battery capacity is  $C_{kb}$ . The completion time of charging  $t_{ikc}$  is shown as equation (7).

$$t_{ikc} = t_{ik} + \frac{(S_{kmax} - S_{kmin})C_{kb}}{\varepsilon P_c} \quad (7)$$

Where  $S_{kmax}$ ,  $S_{kmin}$  are terminal SOC value and initial SOC value of the  $k$ th EV respectively;  $\varepsilon$  is the round-trip energy efficiency;  $P_c$  is the charging power level.

### (2) The upper limit of grid supply power and transformer capacity

The upper limit of grid supply power directly determines the transformer capacity of charging station and the number of EV charging. The power cap of the grid  $P_g$  and the transformer capacity  $P_T$  are constrained by the value of  $\lambda_1$ , as shown in equation (8) and (9):

$$P_g \geq \lambda_1 P_{av} \quad (8)$$

$$P_T \geq \eta_T \lambda_1 P_{ave} \quad (9)$$

Where  $\eta_T$  is the calculation margin of transformer capacity.

### (3) The charge-discharge power of ESS

Set the maximum discharging power of the ESS less than the power cap of the grid, which needs to satisfy the constraint as equation (10).

$$P_b \leq \lambda_1 P_{ave} \quad (10)$$

### (4) The cycle efficiency of ESS

Considering the daily energy of ESS, the cycle efficiency  $w$  needs to meet the constraint as equation (11).

$$w \leq 1 \quad (11)$$

### (5) The number of piles and charging power level

According to the constraint condition of grid power and ESS discharging power, the number of the charging piles  $\theta$  and the power level  $P_c$  are set as equation (12).

$$\lambda_1 P_{ave} + P_b \leq \theta P_c \leq 2\lambda_1 P_{ave} \quad (12)$$

## C. The ESS Capacity

The ESS capacity is calculated with all the ESS charging periods during a day, where the charging time is defined by the valley load period and the PV residual power period. The ESS capacity is also calculated with the ESS discharging periods during a day (When the condition  $\lambda_1 > \lambda_{1max}$  is satisfied, the ESS capacity is constant and determined by the PV residual energy), where the discharging time is defined by the peak load period. The ESS capacity is shown in the follows.

$$E = \frac{\eta_e}{\varepsilon \eta_d} \int_0^{24} \frac{24}{N} (\lambda_2 P_{ave} - P_t + |\lambda_2 P_{ave} - P_t|) / 2 dt \quad (13)$$

$$E = \frac{\eta_e}{w \varepsilon \eta_d} \int_0^{24} \frac{24}{N} (P_t - \lambda_1 P_{ave} + |P_t - \lambda_1 P_{ave}|) / 2 dt \quad (14)$$

Where  $\eta_e$  is the calculation margin of ESS capacity;  $\eta_d$  is the depth of discharging (DOD) of ESS.

## IV. OPTIMIZATION ALGORITHM

### A. NSGA-II Algorithm

Considering the multi-objective, nonlinear and multi-constrained features, the NSGA-II algorithm is adopted.

By analyzing the optimization model,  $\lambda_1$  and  $\lambda_2$  are taken as the decision variables of the optimization function. The flow chart is shown in Figure 3. In order to facilitate algorithm optimization to find the minimum value of the objective function in the solution space, the RMS of the ESS charge-discharge power is taken as a negative value, and the objective function can be simplified as:

$$\{\min(C), \min(-D)\} = f\{\lambda_1, \lambda_2\} \quad (15)$$

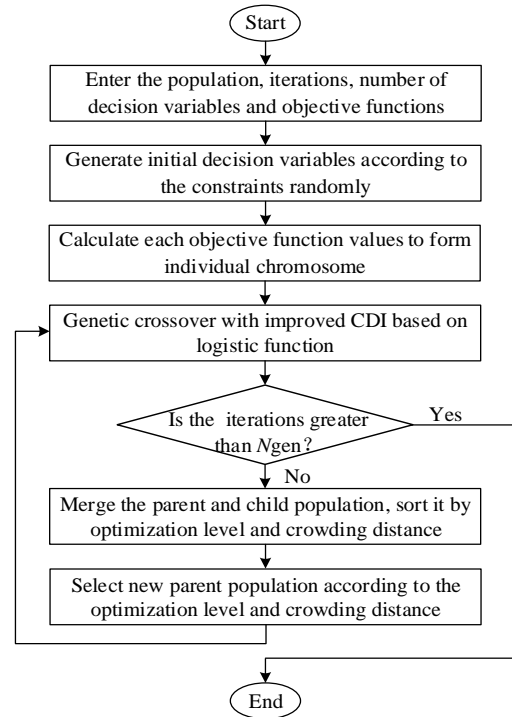


Fig. 3 The flow chart of algorithm optimization

### B. Improve the Genetic Crossover Process

Simulate binary crossover (SBX) is taken as the genetic crossover process method, which mainly imitates the single-point crossover based on binary strings, and is suitable for chromosomes represented by real value.

a. Generating distribution factor  $\beta$  by random number  $u$  ( $0 < u < 1$ ) and CDI  $\eta_c$ .

$$\beta = \begin{cases} (2u)^{\frac{1}{\eta_c+1}}, & 0 < u \leq 0.5 \\ (\frac{1}{2(1-u)})^{\frac{1}{\eta_c+1}}, & 0.5 < u < 1 \end{cases} \quad (16)$$

b. The offspring individuals  $Y_{1,n+1}$  and  $Y_{2,n+1}$  are calculated by the parent individuals  $Y_{1,n}$  and  $Y_{2,n}$ , the correlation coefficient between the distance of the parent individuals

and the distance of offspring individuals is determined:

$$Y_{1,n+1} = 0.5[(1+\beta)Y_{1,n} + (1-\beta)Y_{2,n}] \quad (17)$$

$$Y_{2,n} = 0.5[(1-\beta)Y_{1,n} + (1+\beta)Y_{2,n}] \quad (18)$$

$$Y_{2,n+1} - Y_{1,n+1} = \beta(Y_{2,n} - Y_{1,n}) \quad (19)$$

In the initial stage of crossover, it is not conducive to the decentralized search, which maintains the diversity of the solution by using a constant  $\eta_c$ . It is not conducive to the convergence of the solution in the final stage of crossover. So the logistic function is used to change  $\eta_c(n)$  with the iteration in the evolution process.

$$\eta_c(n) = \frac{\eta_m \eta_0 e^{\gamma \alpha}}{\eta_m + \eta_0 (e^{\gamma \alpha} - 1)} \quad (20)$$

Where  $\eta_0$  is initial value of CDI;  $\eta_m$  is final value of CDI;  $\gamma$  is the coefficient that measures the speed of the curve change;  $\alpha$  is the number of solutions of the first non-dominated layer in the  $n$ th iteration.

## V. CASE ANALYSIS

### A. Basic Parameter Settings

The basic parameters are shown in Table 1.

**Table 1 Basic parameters**

Parameter settings	Parameter value
Discount rate	0.08
Coefficient of transformer annual operation and maintenance	0.01
Coefficient of ESS annual operation and maintenance	0.01
Margin of transformer capacity calculation	1.25
Margin of ESS calculation	1.2
DOD of ESS	0.9
Round-trip efficiency	0.95

**a.** Electricity price. It refers to the Shanghai commercial load time-of-use (TOU) electricity price [14].

**b.** PV output. Considering the PV output of Jiading, Shanghai, integrated with EV charging station, the daily PV output ratio is set at 15% in this paper.

**c.** Power demand for EVs charging. It is assumed that the fast charging power of EV is 120 kW, the daily number of EVs  $N_{ev}$  is 500, the initial SOC value is randomly selected according to Monte Carlo method, the terminal SOC value is 1, and the average size of traction batteries for EV can reach approximately 20~30 kWh. With reference to statistical data about inbound vehicles in the national oil company of Norway [15], the charging power demand is obtained by Monte Carlo simulation.

**d.** The range of decision variables. Considering the actual charging situation, and referring to the constraints of the ESS capacity and the round-trip efficiency, the range of the decision variables  $\lambda_1, \lambda_2$  is set as  $\lambda_1 > 1$  and  $0 < \lambda_2 < 1$ .

### B. The Analysis of Optimization Result

NSGA-II algorithm program is run in MATLAB. Set the population number  $N_{pop} = 200$ , the number of iterations  $N_{gen} = 200$ , the crossover probability  $\rho_{cross} = 0.9$ , the mutation probability  $\rho_{mu} = 0.1$ , the initial value of logistic function  $\eta_0 = 5$ , final value  $\eta_m = 20$  and coefficient  $\gamma = 0.05$ . The distribution of the first non-dominated layer solution is shown in Fig. 4.

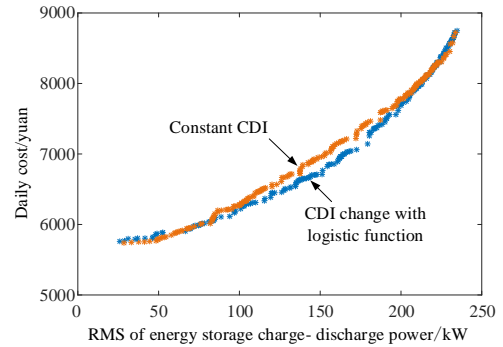


Fig. 4 Distribution of first non-dominated layer solution set

It can be seen that the CDI based on the logistic function has a better optimal solution set and a faster convergence speed in the later stage of evolution comparing with constant CDI, as shown in Fig. 5

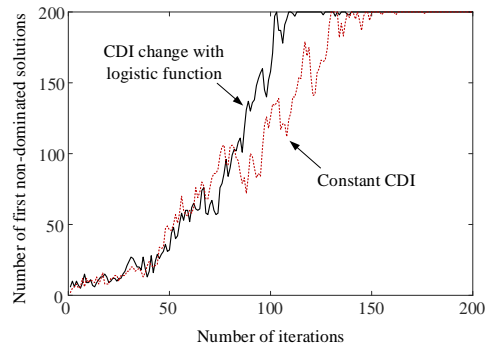


Fig.5 The impact of CDI on optimal solution

In the initial stage of the evolutionary process, a smaller  $\eta_c$  is used to perform a scattered search, which contributes to explore unknown spatial information and maintain the diversity of solutions. As the evolution progresses, the solution tends to converge to Pareto optimal front, which implements a small scale centralized search to improve the convergence speed with a larger  $\eta_c$ .

The distribution of solution set shows that the daily cost increases with the increase of the RMS of ESS charge-discharge power. The minimum daily cost is 5780 Yuan, among which, the ESS capacity is determined by the PV residual power. The maximum daily cost is 8849 Yuan owing to the large ESS capacity.

The daily cost of charging station and the capacity of ESS are calculated with the chromosomes of the first non-dominated layer solution, as shown in Figure 6 and Figure 7.

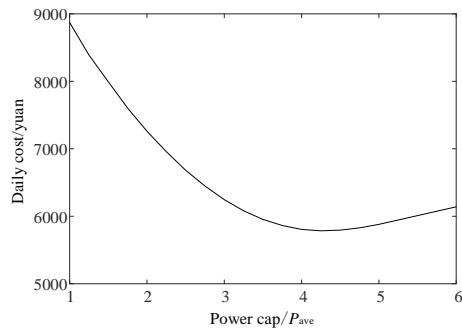


Fig. 6 The impact of power cap of grid on daily cost

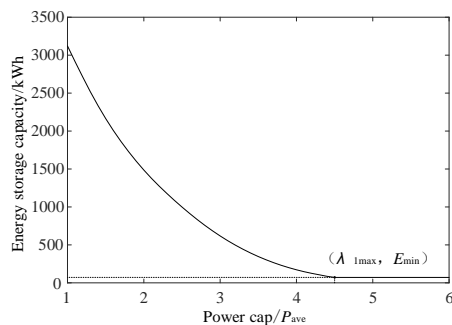


Fig. 7 The impact of power cap of grid on ESS capacity

When the upper limit of grid supply power is higher, the ESS capacity will be required less, and the transformer capacity of the charging station will be larger. When the upper limit of grid supply power is less than 4.27 (the ratio of grid power to average power), the ESS capacity changes greatly. The cost of the ESS capacity reducing is greater than the cost of the transformer capacity increasing. So the cost of the charging station is gradually reduced and the maximum ESS capacity is 3122 kWh. When the upper limit of grid supply power is more than 4.27, the ESS capacity changes little, and the cost of the ESS capacity reducing is less than the cost of the transformer capacity increasing. So the daily cost will increase and the minimum ESS capacity is 70.4 kWh, which is the PV residual energy.

## VI. CONCLUSION

In this paper, a multi-objective ESS capacity configuration model is established to optimize the equivalent load in the mode of peak shaving. NSGA-II algorithm is used to obtain the optimal solution set. The ESS capacity and daily cost at different power levels are analyzed, which provides the initial transformer capacity planning and ESS configuration of the PV integrated with EV charging station. In the process of genetic operator, the CDI

changes the logistic function, and the results show that the algorithm can converge to the optimal solution quickly and better dynamic performance is achieved.

## REFERENCES

- [1] H. Zhang, Z. Hu, Z. Xu, et al, "An integrated planning framework for different types of PEV charging facilities in urban area," *IEEE Transactions on Smart Grid*, vol. 7, pp. 2273-2284, 2016.
- [2] N. Machiels, N. Leemput, F. Geth, et al, "Design criteria for electric vehicle fast charge infrastructure based on Flemish mobility behavior," *IEEE Transactions on Smart Grid*, vol. 5, pp. 320-327, 2014.
- [3] G. R. C. Mouli, P. Bauer, M. Zeman, "System design for a solar powered electric vehicle charging station for workplaces," *Appl. Energy*, vol. 168, pp. 434-443, 2016.
- [4] B. Y. Khanghah, A. A. Moghaddam, J. M. Guerrero, et al, "Combined solar charging stations and energy storage units allocation for electric vehicles by considering uncertainties," *EEEIC/ I & CPS Europe*, Milan, pp. 1-6, 2017.
- [5] N. Saxena, I. Hussain, B. Singh, et al, "Implementation of a grid-integrated pv-battery system for residential and electrical vehicle applications," *IEEE Transactions on Industrial Electronics*, vol. 65, pp. 6592-6601, 2018.
- [6] N. Liu, C. Zheng, J. Liu, et al, "Multi-objective optimization for component capacity of the photovoltaic-based battery switch stations: Towards benefits of economy and environment," *Energy*, vol. 64, pp. 779-792, 2014.
- [7] M. Brenna, A. Dolara, F. Foidelli, et al, "Urban scale photovoltaic charging stations for electric vehicles," *IEEE Transactions on Sustainable Energy*, vol. 5, pp. 1234-1241, 2014.
- [8] P. Zheng, X. Cui, H. Wang, et al, "Research on the accommodation of photovoltaic power considering storage system and demand response in microgrid," *Power System Protection and Control*, vol. 45, pp. 63-69, 2017.
- [9] Y. Zhang, M. E. Haque, M. A. Mahmud, "Control and charge management of a grid-connected photovoltaic system with plug-in hybrid vehicle as energy storage," *IEEE Power & Energy Society General Meeting*, Denver, pp. 1-5, 2015.
- [10] H. F. Su, Z. R. Liang, "Orderly charging control based on peak-valley electricity tariffs for household electric vehicles of residential quarter," *Electric Power Automation Equipment*, vol. 35, pp. 17-22, 2015.
- [11] K. Chaudhari, A. Ukil, K. N. Kumar, et al, "Hybrid optimization for economic deployment of ESS in PV-integrated EV charging stations," *IEEE Transactions on Industrial Informatics*, vol. 14, pp. 106-116, 2018.
- [12] J. Wei, Q. Liu, et al, "Tri-period energy management strategy for PV-assisted EV charging station in residential area," *Electric Power Automation Equipment*, vol. 37, pp. 249-255, 2017.
- [13] K. Mahmud, M. J. Hossain, G. E. Town, "Peak-load reduction by coordinated response of photovoltaics, battery storage, and electric vehicles," *IEEE Access*, vol. 6, pp. 29353-29365, 2018.
- [14] The Grid Sales Price of Shanghai[EB/OL]. [2017-05-15].
- [15] K. Yunus, H. Z. De La Parra, "Distribution grid impact of plug-in electric vehicles charging at fast charging stations using stochastic charging model," *Proceedings of 14th European Conference on Power Electronics and Applications*, Birmingham, 2011.